

## Synchronization in a noise-driven developing neural network

I.-H. Lin, R.-K. Wu, and C.-M. Chen\*

*Department of Physics, National Taiwan Normal University, Taipei, Taiwan*

(Received 18 July 2011; revised manuscript received 19 October 2011; published 29 November 2011)

We use computer simulations to investigate the structural and dynamical properties of a developing neural network whose activity is driven by noise. Structurally, the constructed neural networks in our simulations exhibit the small-world properties that have been observed in several neural networks. The dynamical change of neuronal membrane potential is described by the Hodgkin-Huxley model, and two types of learning rules, including spike-timing-dependent plasticity (STDP) and inverse STDP, are considered to restructure the synaptic strength between neurons. Clustered synchronized firing (SF) of the network is observed when the network connectivity (number of connections/maximal connections) is about 0.75, in which the firing rate of neurons is only half of the network frequency. At the connectivity of 0.86, all neurons fire synchronously at the network frequency. The network SF frequency increases logarithmically with the culturing time of a growing network and decreases exponentially with the delay time in signal transmission. These conclusions are consistent with experimental observations. The phase diagrams of SF in a developing network are investigated for both learning rules.

DOI: [10.1103/PhysRevE.84.051923](https://doi.org/10.1103/PhysRevE.84.051923)

PACS number(s): 87.18.Sn, 87.19.lm, 87.19.lc

### I. INTRODUCTION

Synchronized neural oscillations have been observed in the early stages of many sensory systems of animals, such as insects, frogs, and primates. Studies on lower mammals have demonstrated that synapses between neurons are established from the early developmental stages, and activity-driven synchronization of neurons may occur during development and learning [1,2]. It has been shown that immature pyramidal neurons of the rat hippocampus start to receive sequentially established synaptic inputs around birth [3] and the hippocampal network generates periodic synchronized neuronal discharges during the first two postnatal weeks [4]. Nevertheless it is still unclear whether these neural rhythms contribute to normal functions of brains, are merely epiphenomena, or even interfere with regular physiological processing.

Recently, experimental data has indicated that the synchronization of oscillatory activity seems to be relevant for the development of cortical circuits. This is demonstrated by the involvement of neural synchrony in synaptic plasticity and changes in the synchronization frequency of neural oscillations during development. Mounting evidence from invasive electrophysiology in nonhuman primates, and electro- and magnetoencephalographic (EEG/MEG) recording in humans, has suggested that synchronous oscillatory activities provide a fundamental mechanism for enabling various cognitive and perceptual functions [5–10]. Particularly, it is found that neural rhythms in the beta-gamma range (20–100 Hz) establish precise synchronization of distributed neural responses and play an important role in linking synchronized oscillations to cortical computations. Furthermore, experiments have also suggested that alpha activity (8–12 Hz) is associated with the long-distance coordination of gamma- oscillations, and theta activity (4–8 Hz) supports large-scale integration of subsystems for the formation and recall of memories. In general, there is a correlation between the synchronization frequency

and the distance over which synchronization occurs. In other words, short distance synchronization tends to occur at higher frequencies, while long-distance synchronization occurs at lower frequencies. Although theta frequency oscillations are driven by septal and entorhinal inputs, gamma oscillations are thought to be generated intrinsically [11,12].

It is known that neural networks are replete with various kinds of noise, such as thermal noise, ionic conductance noise, ion channel shot noise, ionic pump noise, synaptic release noise, and synaptic bombardment [13,14]. How neurons can store, process, and compute in such a noisy environment has attracted a great deal of attention. The principle source of noise is assumed typically to be synaptic noise, while thermal noise is rarely considered in neural systems since it is weak in comparison with other sources [15,16]. The possible importance of intrinsic noise from ion channels at the cellular level has been examined both experimentally and computationally [17–20]. These studies have found that, due to the nonlinear response of the system, the addition of noise in a neural network could lead to neural synchrony with or without the presence of a weak external signal. Understanding the evolved mechanism, and the associated nonlinear dynamics that allow neurons to function in a noisy network, is crucial toward understanding information transmission and communication in the brain.

The human brain is one of the most complicated neural networks, which consists of  $10^{11}$  neurons and  $10^{15}$  synapses. Any attempt to simulate a network with such an enormous complexity would not be feasible at the present stage. To investigate the fundamental mechanism of the synchronized oscillations in a developing neural network, a simpler system for computer simulations is culture samples of neural networks, for example, prepared from the cerebral cortex of embryonic rats [21–23]. In this paper, we attempt to study noise-driven synchronized firing (SF) of a developing neural network consisting of 50 neurons. The effects of noise at various developing stages of the network are investigated using the Hodgkin-Huxley (HH) model of neurons. A detailed description of our model is given in Sec. II. In

\*cchen@phy.ntnu.edu.tw

Sec. III, we discuss the main results from our simulations, including the structure of network connections, synchronous activity of neural networks, the synchronization frequency of a developing neural network, and the phase diagram of network synchronization. In Sec. IV, we conclude this study of synchronous behaviors in a noise-driven developing neural network. Stable synchronization can occur in a network with a connectivity greater than 0.73. The synchronization frequency is found to increase linearly with the connectivity, but decrease exponentially with delay time of signal transmission. The phase diagram of network synchronization is investigated by varying the synaptic modification parameters at various stages of network development.

## II. MODEL

To investigate the firing dynamics of a developing neural network, we consider the activity of 50 interneurons, which are randomly grafted on a substrate of area  $L \times L$ , and are not connected to each other initially. The development of the network involves two time scales: at the long time scale ( $T$ , in units of hours), the network gradually builds up synaptic connections between neurons; at the short time scale ( $t$ , in units of 10 ms), neurons communicate with each other through existing connections. The network connectivity is updated every  $10^5$  runs of neuronal communications during our simulations. The probability of forming a synapse between neurons  $i$  and  $j$  is assumed to follow the power law

$$p_{ij} = \frac{k}{r_{ij}^\alpha}, \quad (1)$$

where  $r_{ij}$  is the distance between them. The coefficient  $\alpha$  implies the connection mechanism between two neurons. For  $\alpha = 1$ , the connection between two neurons is built through a random search process, since the connection probability is inversely proportional to the searching circumference of axons. Compared with the random search process, long-distance connections are more favored for  $\alpha < 1$  but less favored for  $\alpha > 1$ . For  $\alpha = 0$ , the developed neural network is a random network, and the connection probability between neurons is independent of their distance. Here we note the value of  $\alpha$  is different in a random connection process ( $\alpha = 0$ ) and in a random search process ( $\alpha = 1$ ). In general, the coefficient  $k$  would depend on, for example, the local concentration of neurotrophins and play roles in regulating neuronal plasticity. Here, for simplicity, we assume a constant  $k = 0.005$  for the entire network at all times. Note that, although we have assumed a simple form of connection probability between two neurons, the exact connection probability is not known experimentally and is probably different for different systems.

In the HH model, the activity of neuron  $i$  in the network is described by a set of four time-dependent variables ( $V_i$ ,  $m_i$ ,  $n_i$ , and  $h_i$ ) [24–26]:

$$C_m \frac{dV_i}{dt} = g_{\text{Na}} m_i^3 h_i (V_{\text{Na}} - V_i) + g_{\text{K}} n_i^4 (V_{\text{K}} - V_i) + g_L (V_{\text{rest}} - V_i) + I_i^{\text{inj}}(t), \quad (2)$$

$$\frac{dm_i}{dt} = (1 - m_i) \frac{25 - V_i}{10 [\exp(\frac{25 - V_i}{10}) - 1]} - m_i \left[ 4 \exp\left(\frac{-V_i}{18}\right) \right], \quad (3)$$

$$\frac{dn_i}{dt} = (1 - n_i) \times 0.1 \times \frac{10 - V_i}{10 [\exp(\frac{10 - V_i}{10}) - 1]} - n_i \left[ 0.125 \exp\left(\frac{-V_i}{80}\right) \right], \quad (4)$$

$$\frac{dh_i}{dt} = (1 - h_i) \times 0.07 \exp\left(\frac{-V_i}{20}\right) - \frac{h_i}{\exp(\frac{30 - V_i}{10}) + 1}, \quad (5)$$

where  $V$  represents the membrane potential,  $m$  and  $h$  are the activation and inactivation variables of the sodium current, and  $n$  is the activation variable of the potassium current. The injected current is a sum of output currents from connected neurons in the network, with a synaptic strength  $w_{ij}$  and a delay time  $T_0$  in signal transmission, which can be expressed as  $I_i^{\text{inj}}(t) = \sum_j w_{ij} I_j^{\text{out}}(t - T_0)$ . For simplicity we approximated the output current  $I_j^{\text{out}}(t - T_0)$  as a step function with a duration 0.1 ms and an amplitude  $I_{\text{max}} \{1 + \exp[-0.002 V_j^{\text{peak}}]\}^{-1}$ , where  $V_j^{\text{peak}}$  is the peak value of the action potential of neuron  $j$  for the outgoing spike near time  $t - T_0$ , and  $I_{\text{max}}$  is the maximum output current from a neuron [27]. Typical values of  $I_{\text{max}}$  and  $T_0$  used in our simulations are 25 nA and 9 ms, respectively. The parameters  $g_{\text{Na}}$ ,  $g_{\text{K}}$ , and  $g_L$  are the maximum conductance per surface area of the sodium, potassium, and leak currents,  $V_{\text{Na}}$ ,  $V_{\text{K}}$ , and  $V_{\text{rest}}$  are the corresponding reversal potentials, and  $C_m$  is the membrane capacitance. Typical values of the parameters in the HH model are  $C_m = 1.0 \mu\text{F}/\text{cm}^2$ ,  $g_{\text{Na}} = 120.0 \text{ mS}/\text{cm}^2$ ,  $g_{\text{K}} = 36.0 \text{ mS}/\text{cm}^2$ ,  $g_L = 0.3 \text{ mS}/\text{cm}^2$ ,  $V_{\text{Na}} = 115.0 \text{ mV}$ ,  $V_{\text{K}} = -12.0 \text{ mV}$ , and  $V_{\text{rest}} = 10.6 \text{ mV}$  [27]. The membrane potential  $V(t + \Delta t)$  in Eq. (2) is solved using the Euler method as

$$V_i(t + \Delta t) = V_i(t) + \frac{\Delta t}{C_m} \{I_{\text{inj}}(t) + g_{\text{Na}} m_i(t)^3 h_i(t) \times [V_{\text{Na}} - V_i(t)] + g_{\text{K}} n_i(t)^4 [V_{\text{K}} - V_i(t)] + g_L [V_{\text{rest}} - V_i(t)]\}, \quad (6)$$

where  $n(t)$ ,  $m(t)$ , and  $h(t)$  can be obtained from solving Eqs. (3)–(5) [27]. We note that the accuracy of membrane potential calculated from Eq. (6) depends on the value of  $\Delta t$ . In our experience,  $\Delta t \leq 0.01$  ms will be a good choice. Here we use  $\Delta t = 0.001$  ms.

Electric noise plays an important role in neuron dynamics. The main source of this noise is typically synaptic, resulting from the probabilistic release of synaptic vesicles and bombardment from the myriad of synapses made by other cells. Although the firing frequency of neurons rarely exceeds 1000 Hz, the combined synaptic activities of a neural network can produce fluctuations on a much faster time scale. Synaptic noise causes abrupt changes in the associated synaptic conductance each time a spike invades the presynaptic bouton. In Stein's model, the effect of noise in the evolution of the membrane potential of a given neuron is described as trains of Dirac delta functions [28]. In the diffusion limit of

synaptic input, the sum of delta functions becomes Gaussian white noise [29,30]. Thus in the presence of synaptic inputs, the membrane potential can be described as

$$\begin{aligned}
 V_i(t + \Delta t) = & V_i(t) + \frac{\Delta t}{C_m} \{ I_{\text{inj}}(t) + g_{\text{Na}} m_i(t)^3 h_i(t) \\
 & \times [V_{\text{Na}} - V_i(t)] + g_{\text{K}} n_i(t)^4 [V_{\text{K}} - V_i(t)] \\
 & + g_L [V_{\text{rest}} - V_i(t)] \} + V_{\text{noise}}, \quad (7)
 \end{aligned}$$

where the Gaussian white noise is generated using  $\sqrt{-2a^2 \ln(\text{rand}) \cos(2\pi \text{rand})}$  with an amplitude  $a = 0.25$  mV and a random variable, rand.

In neural networks, a synapse between two neurons has the ability to change in its strength in response to either use or disuse of transmission over synaptic pathways [31]. Previously, the Hebbian learning rule suggests an increase of the synaptic strength, if the synapse persistently causes the postsynaptic target neuron to generate action potentials (APs). More recent experiments have demonstrated that, in many synapse types, repeated presynaptic spike arrival a few milliseconds (ms) before postsynaptic action potentials leads to long-term potentiation (LTP) of the synapses, whereas repeated spike arrival after postsynaptic spikes leads to long-term depression (LTD) of the same synapse. Previous experiments demonstrated that postsynaptic APs are initiated in the axon, then propagate back into the dendritic arbor of neocortical pyramidal neurons, evoking an activity-dependent dendritic  $\text{Ca}^{2+}$  influx which could be a signal to induce modifications at the dendritic synapses that were active around the time of AP initiation [1]. Therefore the synaptic efficacy can be regulated, depending on the precise timing of postsynaptic APs relative to excitatory postsynaptic potentials. The characteristic time intervals for synaptic modifications are found to be 17 ms for facilitation, and  $-34$  ms for depression for layer 5 pyramidal neurons in the somatosensory cortex [32]. Such a spike-timing-dependent synaptic plasticity (STDP) rule is introduced in our simulations, by considering a change in the synaptic strength due to learning at each time step as [32]

$$\Delta w_{ij}(\Delta\tau) = \begin{cases} A_+ \exp(-\Delta\tau/\tau_+), & \Delta\tau > 0 \\ -A_- \exp(\Delta\tau/\tau_-), & \Delta\tau < 0, \end{cases} \quad (8)$$

where  $\Delta\tau$  is the time of the postsynaptic spike minus the time of the presynaptic spike. The parameters  $\tau_+$  and  $\tau_-$  determine the ranges of pre-to-postsynaptic interspike intervals over which both synaptic strengthening and weakening occur.  $A_+$  and  $A_-$ , which are both positive, determine the maximum amounts of synaptic modification. Typical values of these parameters in our simulations are  $A_+ = 0.0012$ ,  $A_- = 0.0005$ ,  $\tau_+ = 10$  ms, and  $\tau_- = 9.5$  ms. Alternatively, we also consider an inverse STDP rule that has been observed, for example, in the connections between excitatory and inhibitory neurons in the electrosensory lobe of fish [33,34]. These connections are usually seen in sensory systems and cerebral cortex. In this case, the change in the synaptic strength due to learning at each time step is expressed as [33]

$$\Delta w_{ij}^I(\Delta\tau) = \begin{cases} -A_+ \exp(-\Delta\tau/\tau_+), & \Delta\tau > 0 \\ A_- \exp(\Delta\tau/\tau_-), & \Delta\tau < 0. \end{cases} \quad (9)$$

Typical values of these parameters in our simulations are  $A_+ = 0.0005$ ,  $A_- = 0.0012$ ,  $\tau_+ = 10$  ms, and  $\tau_- = 9.5$  ms.

In general, the matrix of synaptic strength is asymmetric. A change in the synaptic strength might result from remodeling of synapses in both presynaptic loci and postsynaptic terminals. Saturation of synaptic efficacy can occur after repeated potentiation, and previous experiments have shown that saturation of hippocampal LTP impairs spatial learning [35,36]. In this paper, for simplicity, we did not introduce saturation for the synaptic efficacy. In our simplified case, the learning due to the external signal is turned off before the synaptic efficacy saturates. We note that several stabilization procedures can terminate learning, either when activity levels reach a certain threshold level, or invoke a bound on synaptic strength [37,38].

For each value of network connections, we simulate the neural activities of the network for 5 s. In the first 2 s, the network is in the learning phase in which the synaptic strength of each connection is updated according to learning rules in Eqs. (8) or (9). Initially, the membrane potential of neurons is chosen to have a Gaussian distribution with a zero average and a standard deviation of 10 mV. The initial synaptic strength between neurons is set to have a Gaussian distribution with an average of 0.05 and a standard deviation of 0.01. After this learning phase, the network enters a so-called recall phase in the last 3 s, in which the learning rule is switched off and the value of synaptic strength remains constant.

### III. RESULTS AND DISCUSSION

#### A. Structure of network connections

For a developing neural network, in our simulations, the general structure of network connections constantly reshapes in the time scale of hours according to Eq. (1). For a culture sample of  $N = 50$  neurons randomly distributed on a square substrate of length  $L$  (in the units of soma size), by fitting those curves of  $N_c$  in Fig. 1, the number of connections ( $N_c$ ) of the network is found to grow logarithmically with time for  $\alpha = 1$ . Here we define the network plating density as  $D = NL^{-2}$ . The time ( $T$ ) for the network to reach a certain number of connections can be well approximated by  $T \propto D^{-\alpha/2}$ . Since experimental measurement of the onset time of SF for cortical neural cultures is proportional to  $D^{-0.44}$  [22], our model with  $\alpha = 1$  seems to describe these neural cultures better.

Furthermore, we calculate the characteristic path length between neurons and average clustering coefficient for various simulated configurations of the neural network. Here the characteristic path length  $l$  is defined to be the minimum number of connections between two neurons. Since neural networks are a directed graph, we define the clustering coefficient of neuron  $i$  as  $C_i = (m_i^2 - m_i)^{-1} \sum_{j,k} e_{jk}$ , where  $m_i$  is the number of neurons connected to neuron  $i$ ,  $e_{jk} = 1$  or 0 if neurons  $j$  and  $k$  are connected or disconnected, and the summation runs over all neurons connected to neuron  $i$ . The average clustering coefficient of the network is defined as  $C_{\text{av}} = N^{-1} \sum_{i=1}^N C_i$ . In the case of  $\alpha = 1$  and  $L = 100$ , we have  $l = 2.91 \pm 0.84$  for  $N_c = 200$ ,  $l = 1.91 \pm 0.32$  for  $N_c = 500$ , and  $l = 1.68 \pm 0.23$  for  $N_c = 800$ . Similarly, the value of  $l$  is 2.88 for  $N_c = 200$ , 1.90 for  $N_c = 500$ , and 1.39 for  $N_c = 1500$  in the case of  $\alpha = 0.5$ , and is 3.12 for  $N_c = 200$ , 1.99 for  $N_c = 500$ , and 1.39 for  $N_c = 1500$  in the

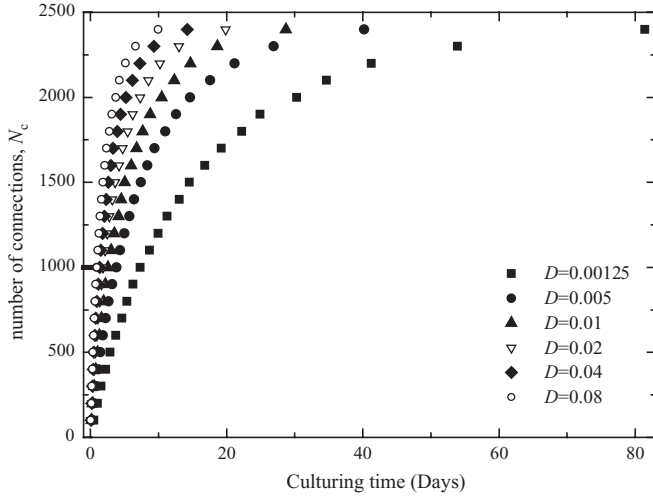


FIG. 1. Number of synaptic connections as a function of culturing time in a growing network with various different plating density  $D$  for  $\alpha = 1$ .

case of  $\alpha = 2$ . This result implies a small separation between neurons in the developing neural networks. In addition, in the case of  $\alpha = 1$ , the average clustering coefficient of the network is calculated to be  $0.110 \pm 0.077$  for  $N_c = 200$ ,  $0.218 \pm 0.029$  for  $N_c = 500$ ,  $0.620 \pm 0.009$  for  $N_c = 1500$ , and  $0.980 \pm 0.001$  for  $N_c = 2400$ . Larger fluctuations in both the characteristic path length and clustering coefficient are observed for neural networks with smaller values of  $N_c$ . The analysis of neural connectivity has revealed that neural networks studied in our simulations exhibit the small-world properties that have been observed in several neural networks. For example, the values of  $(N, J, C_{av})$  are  $(32, 1.69, 0.59)$  for the macaque visual cortex,  $(73, 2.18, 0.49)$  for the macaque cortex,  $(55, 1.79, 0.60)$  for the cat cortex, and  $(282, 2.65, 0.28)$  for *Caenorhabditis elegans* [39].

### B. Synchronous activity of neural networks

Synchronous activity among individual neurons is a robust phenomenon in many regions of the brain [33, 40–42]. To study how synchronization occurs in a noisy environment as a neural network develops, we investigate the correlation in neuronal activities of a network with STDP or inverse STDP learning rules at various developing stages. Here we consider that initially 50 isolated neurons are grafted on a square substrate of size  $L = 100$  and the delay time is set to be 9 ms. Two neurons,  $i$  and  $j$ , are defined to be synchronized if both are active and their time correlation  $\langle TC_{ij} \rangle \equiv \langle [V_i(t) - \langle V_i(t) \rangle][V_j(t) - \langle V_j(t) \rangle] \rangle$ , where angular brackets denote a time average) is greater than 0.2. Furthermore, we define an order parameter  $\Psi_s$  for the synchronization of neuronal activities as the number of synchronized neuron pairs divided by the maximum number of connections ( $N_c^{\max} = 2450$ ). For the case of  $\Psi_s = 1$ , all neurons are synchronized. As shown in Fig. 2, we calculate the order parameter of synchronization,  $\Psi_s$ , for networks at various developing stages with the STDP learning rule. Here the developing stage of a network is described by the number of connections ( $N_c$ ) or by the network connectivity ( $N_c/N_c^{\max}$ ). The value of  $\Psi_s$  is at its background value of about 0.3 for

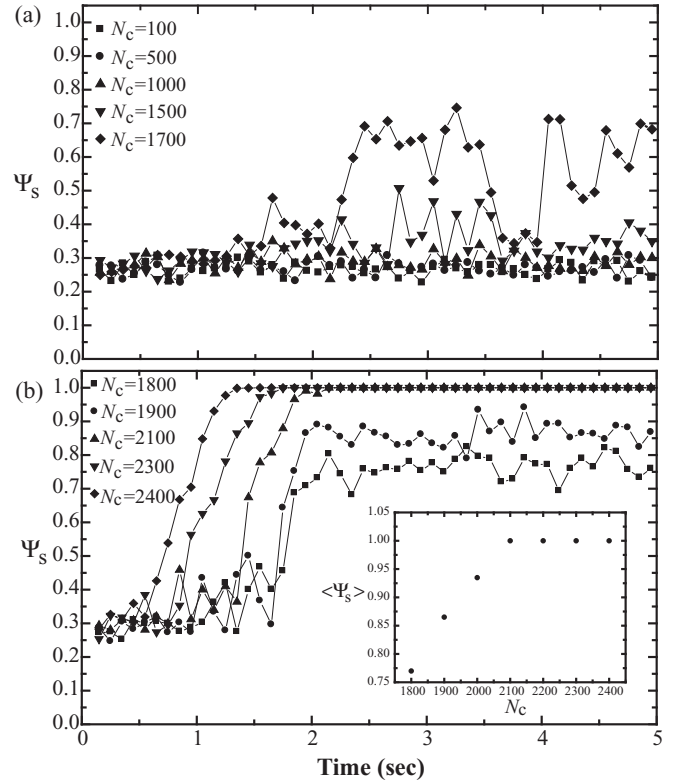


FIG. 2. The time dependence of the order parameter for network SF ( $\Psi_s$ ) in our simulations for neural networks with STDP learning in the case of (a)  $100 \leq N_c \leq 1700$  or (b)  $1800 \leq N_c \leq 2400$ . The inset in (b) shows  $\langle \Psi_s \rangle$  in the recall phase as a function of the number of connections.

$N_c < 1500$ , and starts to fluctuate for  $1500 \leq N_c < 1800$ . For  $N_c \geq 1800$ , the order parameter begins with the background value in the learning phase, and reaches an equilibrium value in the recall phase, which is 0.77 for  $N_c = 1800$ , 0.86 for  $N_c = 1900$ , and 1 for  $N_c \geq 2100$ . This equilibrium value of  $\Psi_s$  ( $\langle \Psi_s \rangle$ , time average of  $\Psi_s$ ) grows linearly from 0.77 to 1 for  $1800 \leq N_c \leq 2100$ , as shown in the inset of Fig. 2(b). All neurons in the network fire synchronously for  $N_c \geq 2100$ . Further investigation shows that the transition from a background activity state to a SF state occurs if the average synaptic strength of the network is greater than 0.04. The time for this transition is about 0.80 for  $N_c = 2400$ , 1.01 for  $N_c = 2300$ , 1.26 for  $N_c = 2100$ , and 1.72 for  $N_c = 1800$ . No transition has been observed for  $N_c \leq 1700$  since the average synaptic strength of these networks is smaller than 0.04 in our simulations. SF can also occur in networks with inverse STDP learning by choosing appropriate parametric values in Eq. (9), in which the relative timing of spikes in a pre- and a postsynaptic cell is reversed. In Fig. 3, we show the synchronization order parameter for a network with the inverse STDP learning rule at various developing stages ( $N_c = 500, 1000, 1700, 1800, 2100$ , and 2400). Similar to the results for networks with STDP learning, there is no enhancement in network synchronization at early developing stages ( $N_c \leq 1700$ ). A steady enhancement of network synchronization is observed for  $N_c \geq 1800$ . For  $N_c \geq 2100$ , all neurons in the network fire synchronously at the network oscillation frequency.

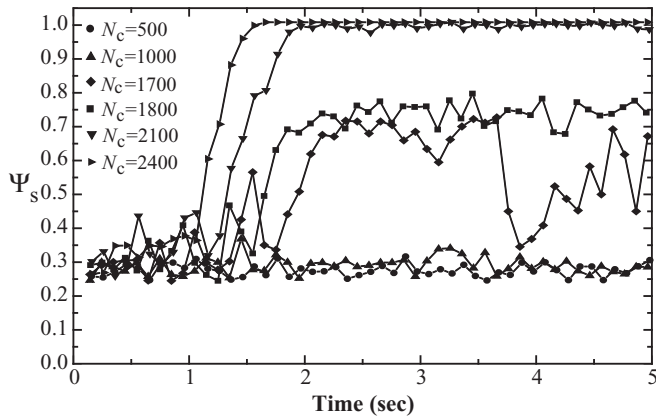


FIG. 3. The time dependence of the order parameter of network SF ( $\Psi_s$ ) in the computer simulations for networks with inverse STDP learning and  $500 \leq N_c \leq 2400$ .

To further study the synchronizing activities of neuron firing at various developing stages, in Fig. 4, we show typical time

series of neuron firing in a network of 50 neurons in the recall phase. For  $N_c \geq 1800$ , synchronous firing of neurons in the neural network is clear. As  $N_c$  increases, more neurons fire synchronously and the time correlation of firing among neurons becomes stronger. In addition, we observe alternate firing in two groups of neurons for  $1800 \leq N_c \leq 2000$ . For  $N_c \geq 2100$ , all neurons in the network fire synchronously. Figure 5 shows various neuronal states in the recall phase for  $N_c = 1800$  [Fig. 5(a)] and for  $N_c = 2400$  [Fig. 5(b)]. In the case of  $N_c = 1800$ , as shown in Fig. 5(a), neurons 1 and 2 belong to the same group of neurons that fire synchronously, while neuron 3 belongs to another group of neurons that fire alternately. Occasionally a number of neurons switch from one synchronous group to another as in the case of neuron 4. As  $N_c$  increases, more neurons switch between these two synchronous groups, and more frequently. When the switching frequency is high enough, the two groups become one synchronous group and all neurons fire synchronously. This phenomenon of overall SF occurs for neural networks with  $N_c \geq 2100$ , and neurons fire at the network frequency. However, for a network with a lesser number of connections,

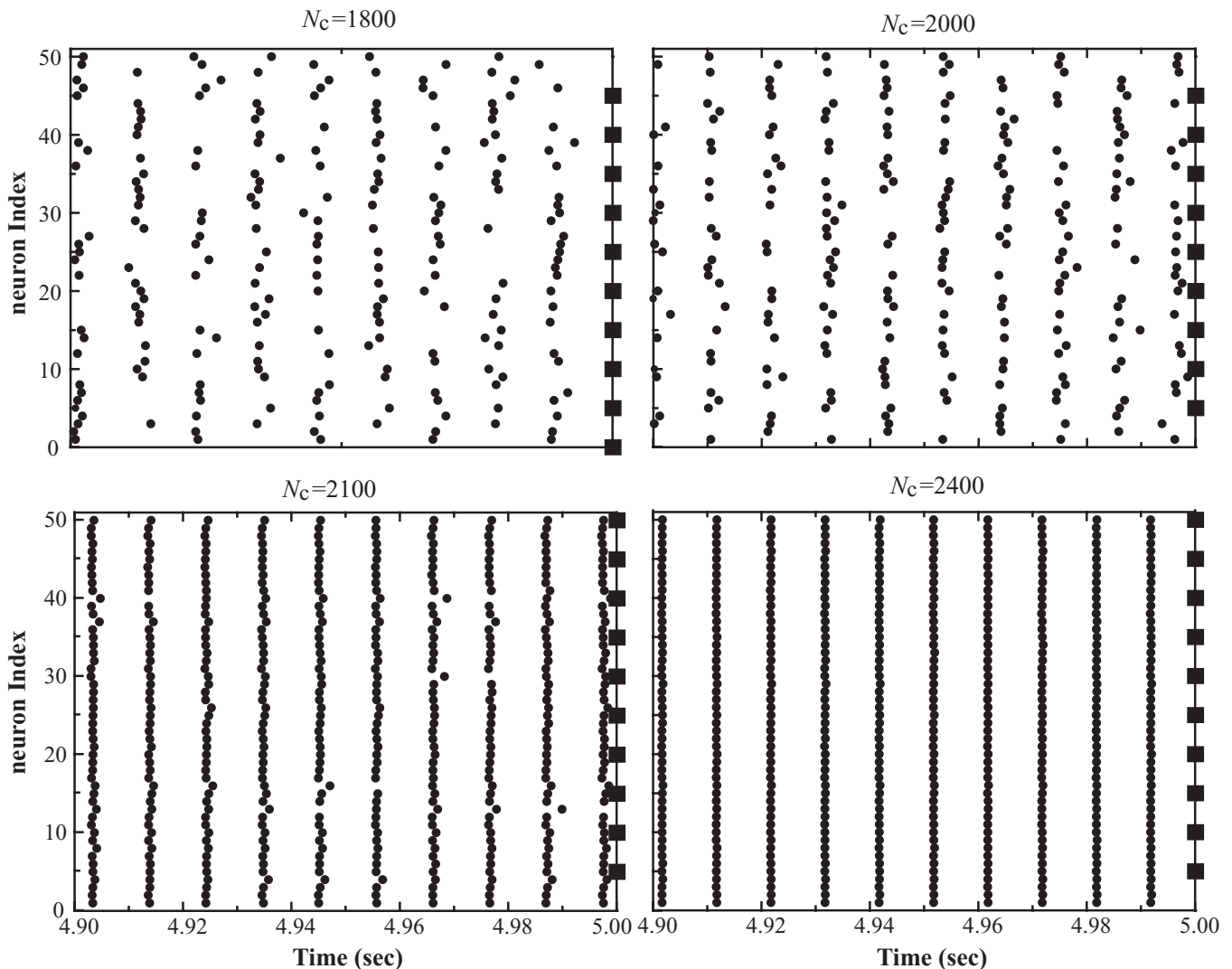


FIG. 4. The firing events of 50 neurons in the recall phase ( $4.9 \leq t \leq 5.0$  s) for networks at different developing stages ( $N_c = 1800, 2000, 2100$ , and  $2400$ ). Clustered SF is observed for  $N_c = 1800$  and  $2000$ , and overall SF is observed for  $N_c = 2100$  and  $2400$ .

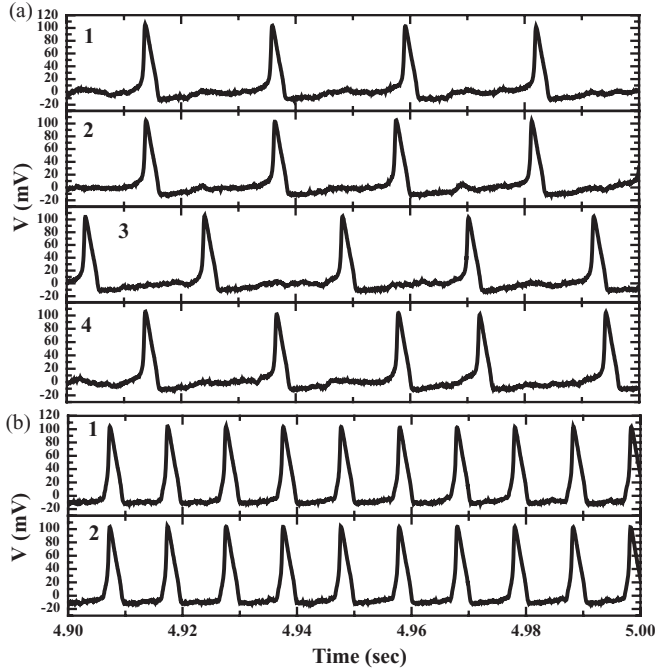


FIG. 5. The time series of membrane potential of four neurons of a neural network with  $N_c = 1800$  in the recall phase (a), and that of two synchronized neurons of a network with  $N_c = 2400$  in the recall phase (b).

the firing frequency of neurons could be considerably smaller than the network frequency when the network breaks in a number of neuron clusters. This type of clustered oscillation has been observed from *in vitro* experiments, in which the network frequency is about 30–40 Hz, and the firing frequency of neurons is less than 2 Hz [43,44].

### C. The synchronization frequency of neural networks

Fast network oscillations (from 40 to 200 Hz) have been observed in both *in vivo* and *in vitro* experiments [44,45]. In Sec. III B, we have demonstrated a fast synchronous oscillation of neural networks that is driven by noise. The SF frequency is found to vary at different developing stages. In Fig. 6, we show the dependence of the synchronization frequency of neural networks on the number of connections [Fig. 6(a)] and culturing time [Fig. 6(b)] of the network for both STDP and inverse STDP learning rules. As shown in Fig. 6(a), fast oscillation is observed for networks with  $N_c \geq 1800$ , and the network oscillation frequency increases linearly with  $N_c$  [22]. Since the number of synaptic connections of a network grows logarithmically with the culturing time of the network as shown in Fig. 1, the network SF frequency is found to increase logarithmically with culturing time in Fig. 6(b). Its time dependence can be fitted to a logarithmic function:  $f = f_0 + c \log(T/T_c)$ , where  $f_0$  is the minimum synchronization frequency,  $T_c$  is the onset time for SF, and  $c$  is a constant. Our simulation results are consistent with recent experimental observations [22], in which a logarithmic time dependence of SF frequency is observed in neuronal culture samples prepared from the cerebral cortex of embryos of Wistar rats. We note,

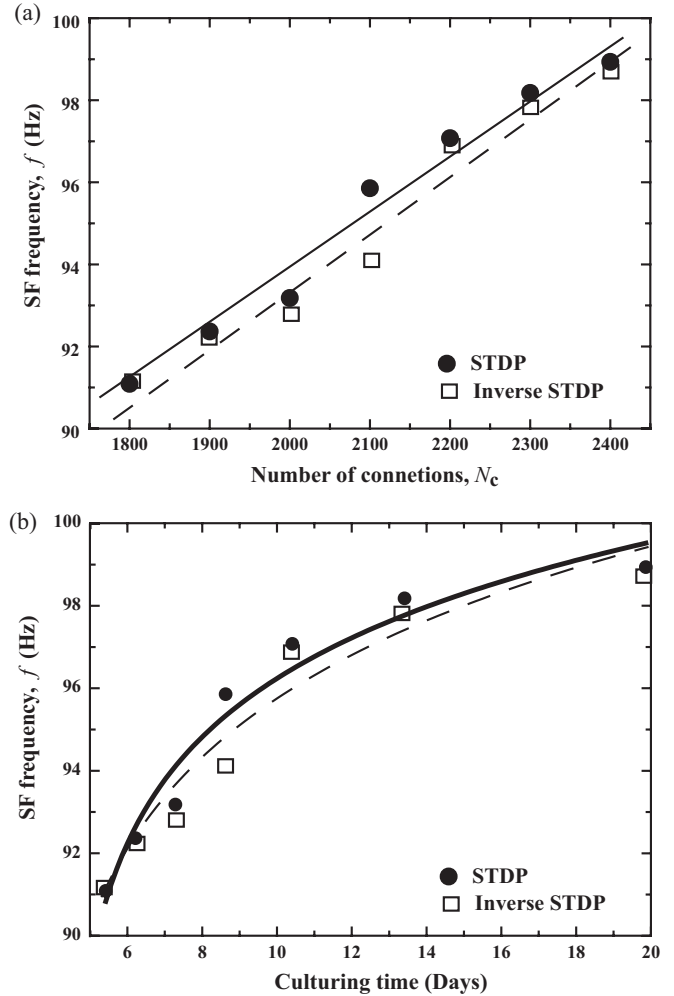


FIG. 6. Network SF frequency as a function of the number of connections (a) and of culturing time (b) for networks with STDP learning or inverse STDP learning.

however, that the characteristic network bursting rate in this experiment is about 1 Hz, which is considerably smaller than the network SF frequency (about 100 Hz) observed in our simulations.

A number of factors could affect the network SF frequency. In our work, we have shown the linear dependence of the SF frequency on network connectivity. Another factor, that could vary the SF frequency, is the strength of noises present in the network. For example, it has been shown that variation in the strength of channel noise could shift the firing rate of neurons from 1000 to 1 Hz [29]. Here we investigate another effect on the network SF frequency resulting from time delay in signal transmission. Time-delayed coupling has been shown to enhance neural synchrony in networks of Hindmarsh-Rose neurons [46]. Similar enhancement of neural synchrony by time delay in signal transmission has also been observed in networks of HH neurons, as shown in Fig. 7. In particular, this enhancement of neural synchrony is most obvious for a network with delay time in the range of 8–20 ms, where the equilibrium order parameter  $\langle \Psi_s \rangle$  reaches its maximal value. Such an enhancement in neural synchrony is due to the increase of synaptic strength under learning

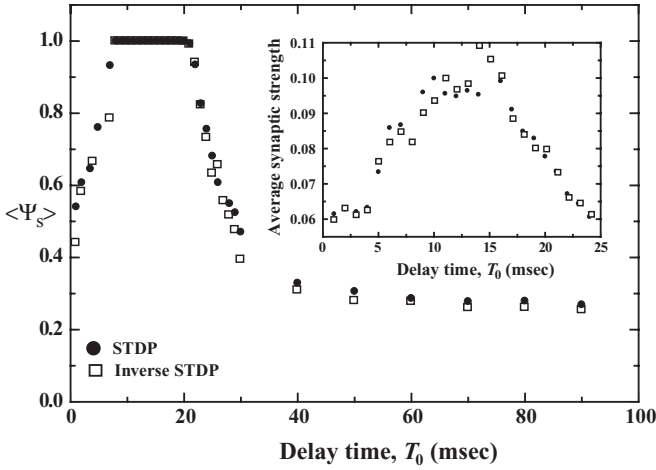


FIG. 7. Time averaged  $\Psi_s$  ( $\langle \Psi_s \rangle$ ) in the recall phase as a function of delay time of signal transmission for neural networks with STDP learning (circles) or inverse STDP learning (squares). The inset shows their average synaptic strength as a function of delay time.

rules in Eqs. (8) or (9). As seen in the inset of Fig. 7, the average synaptic strength of the network has larger values with delay times in the range of 8–20 ms. In addition to the enhancement effect on network synchronization, time-delayed coupling also changes the network SF frequency, as shown in Fig. 8, since signal transmission among neurons takes a longer time for a larger delay time. The data fitting in Fig. 8 shows an exponential decrease of SF frequency with delay time for networks with STDP or inverse STDP learning rules. This delay time in signal transmission is proportional to the distance over which synchronization occurs. Therefore our simulation results are consistent with the experimental observation that short distance synchronization tends to occur at higher frequencies, while long-distance synchronization occurs at lower frequencies.

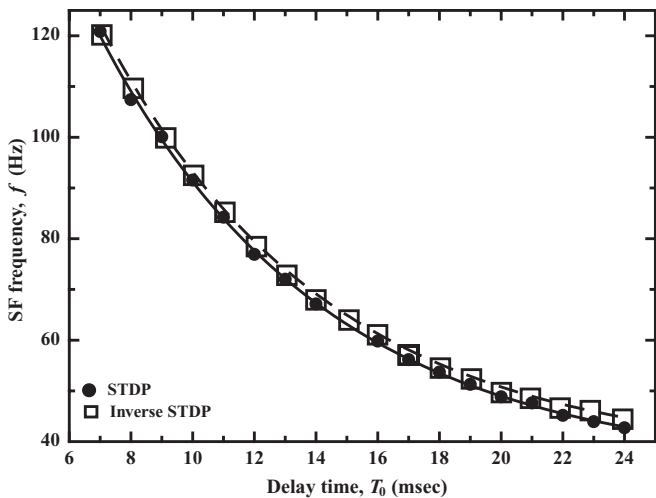


FIG. 8. Network SF frequency as a function of delay time of signal transmission for networks with STDP learning or inverse STDP learning.

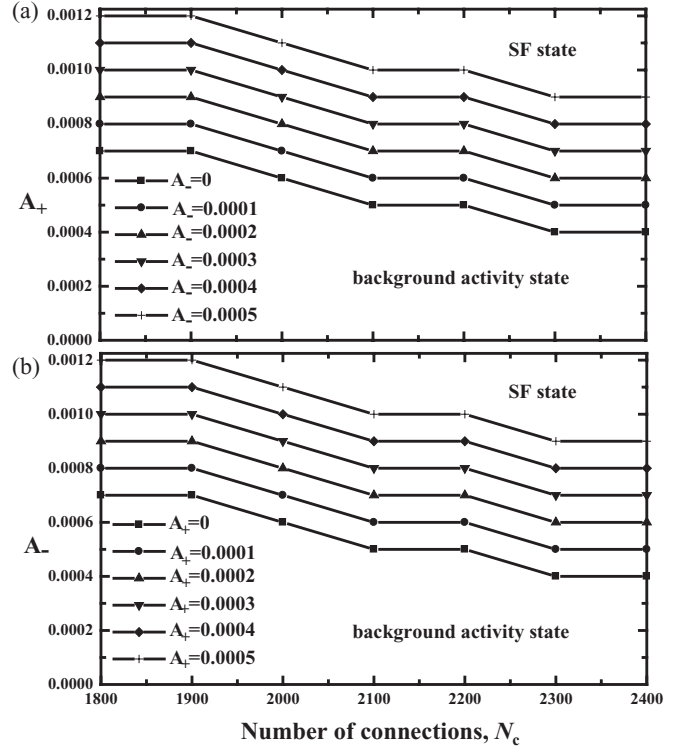


FIG. 9. Phase diagrams of the transition from the background activity state to the SF state, by changing the maximum amounts of synaptic modification,  $A_+$  and  $A_-$ , at various values of  $N_c$  for networks with STDP learning (a) or inverse STDP learning (b).

**D. Phase diagram of network synchronization**

So far, we have demonstrated that SF can be induced by noises in a growing neural network with STDP or inverse STDP learning rules. To observe network SF, we have deliberately chosen appropriate parametric values such that the average network synaptic strength increases with time. For a network of HH neurons, the transition from a background activity state to a SF state can occur for  $8 \leq T_0 \leq 21$  ms and  $N_c \geq 1800$  provided that proper values of  $A_+$  and  $A_-$  in Eqs. (8) or (9) are chosen. The phase diagrams of network synchronization are shown in Fig. 9 for networks with a STDP learning rule [Fig. 9(a)] or an inverse STDP learning rule [Fig. 9(b)], where the delay time is set to 9 ms. For networks with the STDP learning rule, the condition for the existence of a SF state is  $A_+ - A_- \geq 0.7$  for  $N_c = 1800$  and is  $A_+ - A_- \geq 0.4$  for  $N_c = 2400$ . For networks with the inverse STDP learning rule, the condition for the existence of a SF state is  $A_- - A_+ \geq 0.7$  for  $N_c = 1800$  and is  $A_- - A_+ \geq 0.4$  for  $N_c = 2400$ .

**IV. CONCLUSIONS**

In conclusion, we have applied a HH model of neurons to study the noise-driven synchronization behavior in a developing neural network by considering two types of learning rules. The constructed neural networks in our simulations exhibit the small-world properties that have been observed in several neural networks. Stable network SF can occur for networks with  $N_c \geq 1800$  (or network connectivity greater

than 0.73) in the case of  $T_0 = 9$  ms. Our computer simulations show that the network SF frequency increases linearly with network connectivity, and decreases exponentially with delay time of signal transmission. Alternatively, the network SF frequency increases logarithmically with culturing time of a developing neural network, and decreases with the distance over which synchronization occurs. These conclusions are consistent with experimental observations. For  $1800 \leq N_c \leq 2100$ , clustering of neurons in their SF activity is observed and the firing frequency of neurons is only half of the network firing frequency. For  $N_c \geq 2100$  (or network connectivity greater than 0.86), all neurons fire synchronously at the network frequency. The firing activity of the network can be described by an order parameter  $\langle \Psi_s \rangle$ : an overall SF state characterized by  $\langle \Psi_s \rangle = 1$  for  $N_c \geq 2100$ , a clustered SF

state characterized by  $0.75 \leq \langle \Psi_s \rangle < 1$  for  $1800 \leq N_c < 2100$ , and a background activity state characterized by  $\langle \Psi_s \rangle < 0.75$  for  $N_c < 1800$ . Finally, we investigate the phase diagram of network synchronization by varying the values of  $A_+$  and  $A_-$  at various stages of network development. By choosing appropriate parametric values, we show that similar network SF activities can be observed for networks with STDP learning or inverse STDP learning.

#### ACKNOWLEDGMENTS

This work is supported, in part, by the National Science Council of Taiwan under Grant No. NSC 99-2112-M-003-011-MY3. C.M.C. also acknowledges funding support from National Center for Theoretical Sciences of Taiwan.

- 
- [1] H. Markram, J. Lubke, M. Frotscher, and B. Sakmann, *Science* **275**, 213 (1997).
  - [2] Y. Ben-Ari, *Trends Neurosci.* **24**, 353 (2001).
  - [3] R. Tyzio, A. Represa, I. Jorquera, Y. Ben-Ari, H. Gozlan, and L. Aniksztejn, *J. Neurosci.* **19**, 10372 (1999).
  - [4] Y. Ben-Ari, E. Cherubini, R. Corradetti, and J. L. Gaiarsa, *J. Physiol.* **416**, 303 (1989).
  - [5] X. J. Wang, *Physiol. Rev.* **90**, 1195 (2010).
  - [6] J. G. Auerbach, M. Faroy, R. Ebstein, M. Kahana, and J. Levine, *J. Child Psychol. Psychiatry* **42**, 777 (2001).
  - [7] M. J. Kahana, *J. Neurosci.* **26**, 1669 (2006).
  - [8] G. Buzsaki, *Neuron* **33**, 325 (2002).
  - [9] G. Buzsaki and A. Draguhn, *Science* **304**, 1926 (2004).
  - [10] G. Buzsaki, *Hippocampus* **15**, 827 (2005).
  - [11] M. Penttonen, A. Kamondi, L. Acsady, and G. Buzsaki, *Eur. J. Neurosci.* **10**, 718 (1998).
  - [12] M. Bartos, I. Vida, M. Frotscher, J. R. Geiger, and P. Jonas, *J. Neurosci.* **21**, 2687 (2001).
  - [13] P. S. Swain and A. Longtin, *Chaos* **16**, 026101 (2006).
  - [14] W. Gerstner and W. Kistler, *Spiking Neuron Models* (Cambridge University Press, Cambridge, 2002).
  - [15] L. S. Borkowski, *Phys. Rev. E* **83**, 051901 (2011).
  - [16] H. Nguyen and A. B. Neiman, *Eur. Phys. J. Spec. Top.* **187**, 179 (2010).
  - [17] J. A. White, R. Klink, A. Alonso, and A. R. Kay, *J. Neurophysiol.* **80**, 262 (1998).
  - [18] J. A. White, J. T. Rubinstein, and A. R. Kay, *Trends Neurosci.* **23**, 131 (2000).
  - [19] J. T. Rubinstein, *Biophys. J.* **68**, 779 (1995).
  - [20] S. Johansson and P. Arhem, *Proc. Natl. Acad. Sci. USA* **91**, 1761 (1994).
  - [21] T. C. Chao and C. M. Chen, *J. Comput. Neurosci.* **19**, 311 (2005).
  - [22] L. C. Jia, M. Sano, P. Y. Lai, and C. K. Chan, *Phys. Rev. Lett.* **93**, 088101 (2004).
  - [23] J. L. Elman, *Cognition* **48**, 71 (1993).
  - [24] A. L. Hodgkin and A. F. Huxley, *J. Physiol.* **116**, 449 (1952).
  - [25] A. L. Hodgkin and A. F. Huxley, *Cold Spring Harb. Symp. Quantum Biol.* **17**, 43 (1952).
  - [26] A. L. Hodgkin, A. F. Huxley, and B. Katz, *J. Physiol.* **116**, 424 (1952).
  - [27] C. Koch, *Biophysics of Computation* (Oxford University Press, Oxford, 1999).
  - [28] R. B. Stein, *Biophys. J.* **7**, 37 (1967).
  - [29] L. C. Yu, Y. Chen, and P. Zhang, *Eur. Phys. J. B* **59**, 249 (2007).
  - [30] P. Lansky, *J. Theor. Biol.* **107**, 631 (1984).
  - [31] J. R. Hughes, *Physiol. Rev.* **38**, 91 (1958).
  - [32] G. Bi and M. Poo, *Annu. Rev. Neurosci.* **24**, 139 (2001).
  - [33] V. P. Zhigulin, M. I. Rabinovich, R. Huerta, and H. D. Abarbanel, *Phys. Rev. E* **67**, 021901 (2003).
  - [34] C. C. Bell, V. Z. Han, Y. Sugawara, and K. Grant, *J. Exp. Biol.* **202**, 1339 (1999).
  - [35] C. A. Castro, L. H. Silbert, B. L. McNaughton, and C. A. Barnes, *Nature (London)* **342**, 545 (1989).
  - [36] E. I. Moser, K. A. Krobert, M. B. Moser, and R. G. Morris, *Science* **281**, 2038 (1998).
  - [37] M. M. Nass and L. N. Cooper, *Biol. Cybern.* **19**, 1 (1975).
  - [38] R. Linsker, *Proc. Natl. Acad. Sci. USA* **83**, 7508 (1986).
  - [39] S. Boccaletti, V. Latora, Y. Moreno, M. Chavez, and D. U. Hwang, *Phys. Rep.* **424**, 175 (2006).
  - [40] W. M. Usrey and R. C. Reid, *Annu. Rev. Physiol.* **61**, 435 (1999).
  - [41] M. C. Tresch and O. Kiehn, *J. Neurosci.* **22**, 9997 (2002).
  - [42] T. Nowotny, V. P. Zhigulin, A. I. Selverston, H. D. Abarbanel, and M. I. Rabinovich, *J. Neurosci.* **23**, 9776 (2003).
  - [43] A. Fisahn, F. G. Pike, E. H. Buhl, and O. Paulsen, *Nature (London)* **394**, 186 (1998).
  - [44] J. M. Fellous and T. J. Sejnowski, *Hippocampus* **10**, 187 (2000).
  - [45] J. Csicsvari, H. Hirase, A. Czurko, A. Mamiya, and G. Buzsaki, *J. Neurosci.* **19**, 274 (1999).
  - [46] M. Dhamala, V. K. Jirsa, and M. Ding, *Phys. Rev. Lett.* **92**, 074104 (2004).